ELSEVIER

Thermochimica Acta 337 (1999) 155–161

thermochimica acta

www.elsevier.com/locate/tca

Crystallization kinetics of amorphous silicon carbide derived from polymeric precursors

Dirk Kurtenbach[a,*], Brian S. Mitchell[b], Haoyue Zhang[b], Martin Ade[a], Eberhard Müller[a]

[a]*University of Mining and Technology Freiberg, Institute of Ceramic Materials, Gustav-Zeuner-Str. 3, D-09596 Freiberg, Germany*
[b]*Tulane University, Department of Chemical Engineering, New Orleans, LA, USA*

Received 30 April 1999; received in revised form 22 June 1999; accepted 7 July 1999

Abstract

Phase separation processes like nucleation, crystallization and degradation of a polymer-derived amorphous silicon carbide precursor were quantified by means of thermoanalytical methods (DTA/TG). It is shown that the crystal size of the nanostructure could be controlled and limited by nuclei-inducing heat treatments. Furthermore, the justification for application of the JMAK theory was partially given. A comparison to amorphous SiC processed by other means (ion implanted) was drawn and reveals surprising similarities. © 1999 Elsevier Science B.V. All rights reserved.

Keywords: Nucleation; Crystallization; Degradation; Amorphous SiC; Crystal size control

1. Introduction

Manufacturing of non-oxide ceramic materials from the pyrolytic or thermolytic degradation of polymeric precursors (here: silicon-organic compounds) is an alternative route to the conventional, more classical, powder ceramic technology [1]. The main advantages of this route are (1) low pyrolysis temperature, (2) high purity and (3) homogeneous distribution of the participating atoms on a molecular level [2]. Special attention has been given to the design of nano- or microcrystalline structures by adjusting processing parameters, i.e. temperature, time, quench rate or by introducing heteroatoms into the polymer structure by means of chemical modifications [3].

Recent trends in the development of ceramic matrix composites for high temperature applications in aerospace, aviation or traffic technologies, have revealed that silicon carbide-containing composites fulfill the demands for high temperature stability, light weight construction and oxidation resistance [4]. Both the production of SiC-fibres as well as the manufacturing of SiC-matrices proceed via the polymer route, i.e. by means of the pyrolytic degradation of reactive polysilanes or polycarbosilanes.

In order to control the structure of the inorganic product (like fibres, matrices, coatings etc.) it is desirable to gain insight into the kinetics of the phase separation processes such as nucleation, crystallization and, potentially, degradation. Besson et al. [5] have shown successfully that the limitation of crystal

*Corresponding author. Present address: Federal Institute of Materials Research and Testing, Unter den Eichen 87, D-12200 Berlin, Germany. Fax: +49-3081041527
E-mail address: dirk.Kurtenbach@bam.de (D. Kurtenbach)

0040-6031/99/$ – see front matter
PII: S0040-6031(99)00230-0

sizes of a former amorphous intergranular phase (Y–Si–Al–O–N), followed by an improvement of mechanical properties, is possible due to a thermal treatment by inducing many nuclei which restrict crystal growth at higher temperatures. Therefore, an understanding of the aforementioned processes is essential, in particular the maximum nucleation and crystallization temperatures.

The purpose of this work is to determine nucleation and crystallization kinetics of amorphous $SiC_xCl_yH_z$ through thermoanalytical methods such as differential thermal analysis (DTA) and thermogravimetric analysis (TG), and to give evidence that the crystal size may be influenced by appropriate thermal treatments at the maximum nucleation temperature, $T_{n_{max}}$. This will be a powerful tool in the selection of pyrolysis parameters that lead to nanocrystalline materials such as fibres or matrices with improved mechanical properties (strength, creep resistance, etc.). The applicability of the classical theory by Johnson–Mehl–Avrami–Kolmogorov to polymer-derived SiC [6–8], is discussed and similarities or differences with oxidic glasses are shown.

2. Experimental

Amorphous, chlorine-containing SiC powders were produced by thermolysis of a organosilane precursor (Polychloromethylsilane, PS). The starting precursor was a solid granulate with a density of approximately 1 g cm^{-3}. This granulate was ground to a fine powder and subsequently placed in a carbon vessel. This procedure was carried out in an argon-filled glove box in order to avoid oxygen impurities.

The thermolysis was performed in an alumina tube furnace in flowing argon (99.9990%, 15 l_{Ar} min^{-1}) at 973 K for 1 h with heating and cooling rates of 2 K min^{-1}. The as-received SiC was ground and sieved into two powder fractions (<50 μm and 200–315 μm). In order to avoid impurities coming from abrasion, grinding was performed in a silicon carbide mortar. The coarse powder fraction was subjected to further heating in the temperature range from 1173 to 1473 K (50 K steps).

Density measurements of these intermediates were carried out by means of a helium pycnometry apparatus from Micromeritics (AccuPyc 1330 Pycnometer for 1 cc samples). Analyses of oxygen, nitrogen and free carbon of the intermediates have been performed using combustion methods with a LECO apparatus (RC 412 for carbon determination, TC 436 for oxygen/nitrogen determination).

The transformation process from the amorphous pre-pyrolyzed powder to nanocrystalline SiC was analyzed on a TA Instruments simultaneous differential temperature–thermogravimetric analyzer (SDT) 2960 using Pt pans and ca. 40 mg sample sizes. The DTA-unit was calibrated for melting point using silver and for baseline using a standard instrument software routine.

Gas evolution from the SDT was monitored by a quadrupole mass spectrometer (QMS, FISONS Instruments VG Gas analysis systems). In order to determine the activation energy of the crystallization process SDT (DTA/TG) experiments with different heating rates (Q = 5, 10, 15, 20, 30 and 40 K min^{-1}) to a maximum temperature of 1773 K in flowing argon (110 ml_{Ar} min^{-1}) on the fine fraction pre-pyrolyzed powder (<50 μm) were carried out. The nucleation experiments were carried out in the same SDT (DTA/TG) with a unique heating rate (40 K min^{-1}) up to 1773 K and dwell times of 3 h at different nucleation temperatures (T_n = 973–1273l, 50 K steps) in accordance with the work in [9]. The high heating rate (40 K min^{-1}) was chosen in order to avoid additional formation of nuclei above T_n during the DTA experiment. The use of the coarse powder fraction should further avoid or reduce surface nucleation from T_n that potentially may affect the results.

XRD analyses on the DTA residuals were performed on a X-ray diffractometer (Scintag XDS 2000) with Cu K_α adiation. Mean grain sizes were determined using the Scherrer and Wilson equations from the breadth of the β-SiC [2 2 0] diffraction lines. The morphological characterization of the crystallized SiC samples was carried out on a conventional and analytical transmission electron microscope (TEM, Philips CM-200). The samples for TEM observations were ground and picked up on a copper grid in alcohol.

The usual method for obtaining kinetic data involves a series of experiments carried out under isothermal conditions at different temperatures. This process is time and material consuming, see [10]. DTA techniques are dynamic methods that allow one to determine kinetic data (e.g. activation energy, E, and

reaction order, n) as well as the nucleation behaviour of amorphous systems [11].

3. Stoichiometry

The stoichiometry of the starting polymer granulate is well described by the chemical formula $SiCH_3Cl_{0,5}{\cdot}0.25C_8H_8$. The low styrene content (C_8H_8) of the polymer is advantageous in regard to the spinnability of the polymer melts to produce SiC-fibres [32].

Due to the release of oligomers such as chlorine, hydrogen, and methane, the chemical composition of the pre-pyrolyzed (973 K for 1 h) amorphous inorganic powder changes to $SiC_xCl_yH_z$ with x =1.1–1.2, $y = 0.1$ and $z = 0.5$–0.9. Further heating to temperatures beyond the crystallization temperature leads to near stoichiometric SiC with small amounts of excess carbon (SiC_x with $x = 1.05$–1.15) [12]. Small oxygen impurities in the intermediates may be attributed to impurities of the carrier gas and leakage of the tube furnace. However, the uptake oxygen from the environment strongly depends on the temperature at which the intermediate was treated. Only small amounts of oxygen were detected below 1223 K (< 0.5 wt%), whereas amounts of 2.0–3.0 wt% were found at temperatures from 1223 to 1273 K. As a consequence the incorporation of oxygen during the DTA experiments could not be totally avoided, even under flowing argon. Larger argon flow rates could have reduced the level of oxygen impurities, but would have made off-gas mass spectrometry impossible.

4. Kinetic results

The calculation of the kinetic data (activation energy, E, reaction order, n, nucleation temperature, T_n, and crystallization temperature, T_c) by means of non-isothermal experiments e.g. within a dynamic DTA measurement applying the classical theory of Johnson–Mehl–Avrami–Kolmogorov (JMAK) is justified, if the temperature range is very small and an Arrhenian temperature dependence of both nucleation and crystal growth can be assumed. The validity of this assumption has been shown for many glass systems (mainly oxides) by comparing so derived kinetic data with results from classical isothermal methods, see [9,13,14].

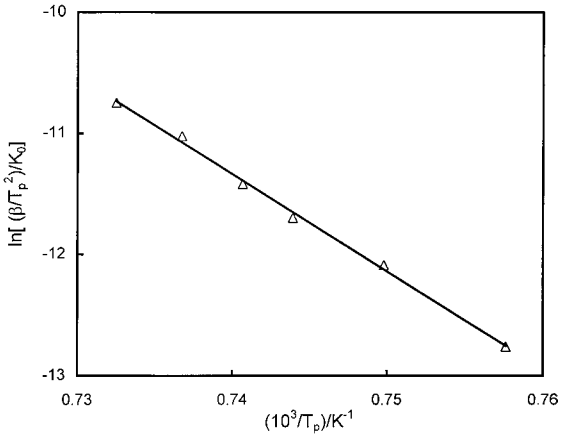

Fig. 1. Kissinger plot, the slope of the straight line yields a activation energy for the SiC crystallization of 667 ± 20 kJ mol^{-1}.

4.1. DTA/TG experiments to determine ΔE

The results of the SDT DTA/TG experiments with different heating rates (β), that are not separately illustrated, are presented in a Kissinger plot (Fig. 1) in accordance with the well known Kissinger Eq. (1) [15]:

$$\ln\frac{(\Delta E{\cdot}\beta)/RT_p^2}{k_0} = -\frac{\Delta E}{RT_p}, \quad (1)$$

where β (K s^{-1}) is the heating rate, T_p (K) the maximum temperature of the exothermic crystallization peak, which varies depending on β, k_0 the frequency factor (s^{-1}) and R the gas constant with 8.314 J/K·mol.

Eq. (1) is only valid if surface crystallization on a fixed number of nuclei proceeds during the DTA run, otherwise a corrected equation has to be used [16]. Therefore, the fine powder fraction (<50 μm) was used for these experiments in order to fulfill the above mentioned demand.

Using Eq. (1), the activation energy of the SiC crystallization can be determined from the slope of the straight line in Fig. 1 as 667 ± 20 kJ mol^{-1}. At temperatures at and above 1673 K a second exothermic peak appears with much smaller intensity. The activation energy of this process, believed to be due to the recrystallization of SiC [17], is calculated in the

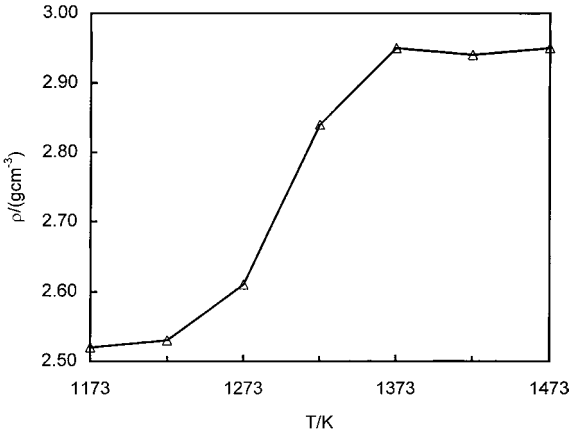

Fig. 2. Density (ρ) measured on intermediates with increasing annealing temperature.

same way described above as 381 ± 20 kJ mol^{-1} [33]. Further evidence that the observed first exothermic peak is attributed to the crystallization of SiC from an amorphous random network is given by density measurements of the intermediates (see Fig. 2) that show a strong increase in density between 1273 and 1373 K from 2.61 ± 0.01 to 2.95 ± 0.01 g cm^{-3}. The TG traces (see Fig. 3) show no significant mass loss at this temperature. These observations clearly identify the exothermic peak as the SiC-crystallization event that is in conjunction with a densification of the system without appreciable mass loss.

The Avrami parameter was calculated as $n = 1.0 \pm 0.1$, using Ozawa's method [18] so that the application of the Kissinger Eq. (1) is justified, because this value means surface crystallization.

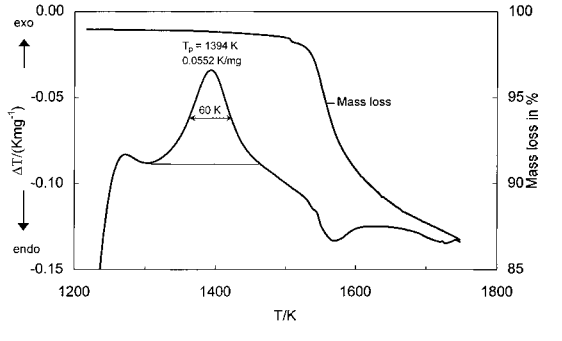

Fig. 3. Simultaneous DTA/TG trace with 3 h nucleation dwell time at 1223 K (heating rate: 40 K min^{-1}). The unit K mg^{-1} that the values were normalized by the individual sample weight.

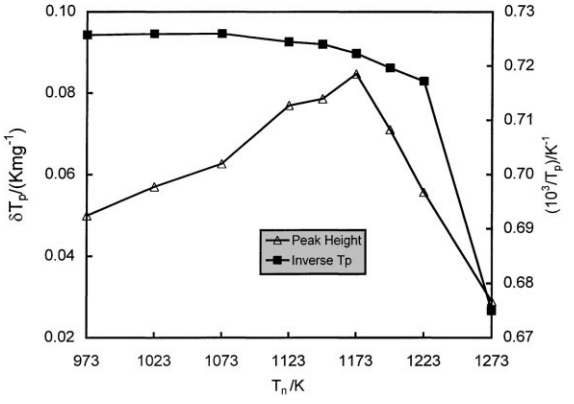

Fig. 4. Peak height and inverse T_p over nucleation temperature (T_p) calculated from DTA experiments. The unit K mg^{-1} means that the values were normalized by the individual sample weight.

4.2. DTA/TG experiments to determine $T_{n_{max}}$

An example for a DTA/TG trace with dwell time for 3 h at 1223 K is depicted in Fig. 3. Again, the SiC crystallization process is clearly identified by an exothermic peak with $T_p = 1394$ K. The results of the nucleation experiments are presented in Fig. 4.

According to Marotta [10,19] both T_p and the intensity of the crystallization, characterized by the peak height (δT_p), should give a bell shaped function, i.e. curvature with a maximum, of T_n. Marotta has shown, that the larger the number of nuclei, the lower the crystallization temperature (T_p, maximum growth rate, [20]). The Marotta formula, Eq. (2):

$$T'_p - T_p = c_1 \ln N_H + c_2 \quad (2)$$

(with T'_p the maximum peak temperature of a DTA experiment without nucleation dwell time) indicates that the higher the difference of $T'_p - T_p$ the higher the number of nuclei (N_H) that has been formed during the dwell time.

From classical glass theory it is well known that the nucleation rate shows a bell shaped temperature dependence. Therefore, the inverse of $T_p\left(T_p^{-1}\right)$ as a function of T_n should give a bell shaped function, too, because at temperatures where the nucleation rate is low, T_p^{-1} is low too and vice versa. The maximum of this function characterizes $T_{n_{max}} \cdot T_p^{-1} = f(T_n)$ did not show the expected behaviour. In contrast, the function of the maximum peak height (δT_p) over T_n shows the expected behaviour resulting in $T_{n_{max}} = 1173 \pm 50$ K

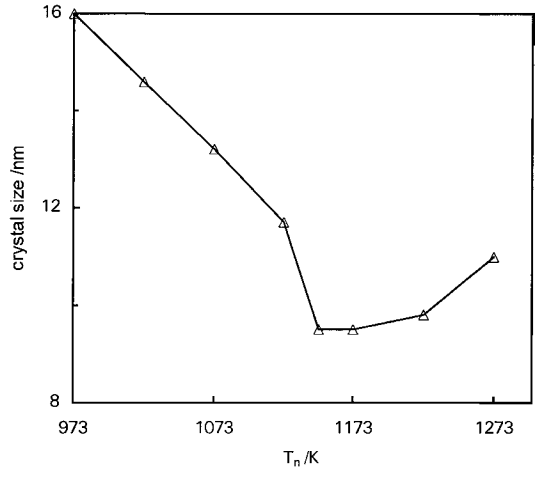

Fig. 5. Crystal sizes determined by means of X-ray peak line broadening in dependence on nucleation temperature (T_n).

This value of $T_{n_{max}}$ is consistent with more qualitative investigations of other authors [21].

In order to confirm the determined $T_{n_{max}}$, X-ray investigations of the DTA residuals were carried out. The results of these investigations are given in Fig. 5. Actually, the assumption that heat treatments at $T_{n_{max}}$ lead to structures with lower crystal sizes is proven because samples that were annealed near $T_{n_{max}}$ (i.e. 1148–1223 K) reveal the lowest crystal sizes (around 9 ± 1 nm) of all samples. TEM investigations of the residuals confirm the X-ray diffraction results. These observations confirm both:

1. high nucleation rates in the range 1123–1198 K with $T_{n_{max}}$ at 1173 K;
2. the effectiveness of a thermal treatment at $T_{n_{max}}$ with regard to the limitation of crystal sizes due to spatial (little space available for each nucleus to grow) and elemental (the atoms needed for crystal growth are not available in the proper stoichiometric ratio) constraints.

The TG trace in Fig. 3 reveals that at temperatures where crystallization is nearly completed (around 1500 K) a strong mass loss occurs that reaches a value of nearly 14 wt% at 1750 K. The QMS (quadrupole mass spectrometer) shows a strong signal for chlorine after 1373 K, i.e. after crystallization. The chlorine content of the pre-pyrolyzed precursor (973 K, 1 h) was determined by means of chemical analyses as $3–5 \pm 1$ wt% as a maximum. Therefore, the release of all residual chlorine atoms could not be the only explanation for the total mass loss of about 14 wt%. In addition there is a release of remaining hydrogen atoms as pointed out by Martin [22] in his investigations but to a small extent because the signal for $m/z = 2$ did not appear in the QMS. The mass loss can be further attributed to the following processes [33]:

An active oxidation of the reactive, nanocrystalline SiC due to low oxygen partial pressure (see [24,25]), indicated by a QMS signal at $m/z = 32$ due to carrier gas impurities whereas the amorphous SiC shows good resistance against oxidation because the inner surface of the amorphous network is very small [22]. This causes further mass loss by the evolution of $SiO_{(g)}$ and $CO_{(g)}$ [23] because the oxygen partial pressure is too low to lead to passive oxidation that generates a protective silica layer around the particles. Evidence for this is given by an increase of the $m/z = 44$ QMS signal at temperatures above 1473 K originated by $SiO_{(g)}$ and $CO_{2(g)}$.

Combustion of excess carbon which is precipitated in an free carbon phase and therefore available for environmental oxygen after crystallization of SiC (see Section 3). Combustion analyses (LECO) of the intermediates show significant amounts of free carbon (around 5 ± 1 wt%) in the samples heated above 1373 K (after SiC crystallization) whereas the lower temperatures intermediates did not show any significant amount of free carbon (<0.1 wt%) because the carbon is incorporated into an amorphous network and protected against the combustion due to analysis oxygen [22].

Calculations of the Avrami exponent (n) for the nucleation experiment with a 3 h dwell time at 1173 K, analogous to the procedure of Ozawa [18], give a value of 1.4 ± 0.1 (i.e. near 1.5) indicating that diffusion controlled growth governs the crystallization process from a nearly fixed number of nuclei [10]. Obviously a nucleation treatment of 3 h is sufficient to lead to a saturation with nuclei and this confirms the applicability of the JMAK theory and their modifications.

5. Discussion

The precipitation of excess carbon in a free carbon phase due to the crystallization of SiC

$$\text{am.-SiC}_{(1+x)} \overset{>1373\,\text{K}}{\Rightarrow} \text{cryst.-SiC}_{(s)} + x\text{C}_{(s)} \qquad (3)$$

and the subsequent combustion of this free carbon due to oxygen impurities of the carrier gas contributes to the observed mass loss of nearly 14 wt%.

Further knowledge of nucleation and/or crystallization processes arises from research work carried out on amorphous SiC processed by amorphization of crystalline SiC by means of ion implantation [27]. Although this represents a totally different processing route compared to the current polymer route the results are surprisingly very similar. In [28] the crystallization temperature was reported as 1348 ± 25 K and the nucleation temperature was observed by means of TEM investigations at $T_n = 1173$ K. These values are in excellent agreement with results of the current work. Moreover, in [29] the activation energy (E) for solid phase and random nucleated crystallization for silicon (Si) in covalent semiconductors was determined as 3.0–4.0 eV. This fits well with the calculated value for the activation energy of the first crystallization event ($667\,\mathrm{KJ\,mol^{-1}} \hat{=} 3.46\,\mathrm{eV/atom}$). Obviously, the structure of amorphous SiC is independent of the processing route or the prehistory of the material.

Furthermore, it has been shown that classical glass theories (JMAK) are, within limitations, valid for the crystallization kinetics of precursor derived amorphous SiC systems. However, there are still existing questions, e.g. why did not the $T_p^{-1} = f(t_n)$ function show the expected bell shaped relationship, even though δT_p revealed the expected nucleation-temperature behaviour? It seems that the densification of the amorphous network due to relaxation processes (rearrangements) hinder diffusion-controlled nucleation and crystal growth, whereas classical glassy systems support such processes due to a decrease in density (above T_g) and viscosity with increasing temperature. Another aspect is the expected change in specific surface area that may increase the non-desired contribution of surface nuclei formed during nucleation.

6. Conclusions

The current investigation completes and confirms recently presented investigations on SiC derived from other polymeric precursors [21,26,30,31,33]. For the first time processes like nucleation, crystallization and recrystallization in polymer derived SiC system have been quantified [33]. Furthermore, it has been shown that DTA experiments are a useful tool for the investigation of crystallization kinetics in precursor-derived SiC. The obtained data provides a good basis for the adjustment of microstructure by thermal treatment, leading, potentially, to improved mechanical properties of poly(chloromethylsilane) derived SiC materials.

Acknowledgements

Acknowledgement is made to the ''Graduiertenkolleg Werkstoffphysikalische Modellierung'', an institution of the ''Deutsche Forschungsgemeinschaft (DFG)'' at the University of Mining and Technology Freiberg (Germany, Saxony), for financial support to carry out the research work and to the ''Deutsche Akademische Austauschdienst (DAAD)'' for a Study Grant Award.

References

[1] R. Riedel, Mater. Sci. Technol. 17B (1996) 1.
[2] J. Bill, F. Aldinger, Adv. Mater. 7 (1995) 775.
[3] J. Lücke et al, cfi/Ber. DKG 75 (1998) 18.
[4] A. Mühlratzer, cfi/Ber. DKG 76 (1999) 30.
[5] J.-L. Besson et al., J. Non-Crysst. Sol. 211 (1997) 1.
[6] W.A. Johnson, R.F. Mehl, Trans. Metall. Soc. AIME 135 (1939) 416.
[7] M. Avrami, J. Chem. Phys. 7 (1939) 1103.
[8] A.N. Kolmogorov, Izv. Akad. Nauk. USSR Ser. Mat. 1 (1937) 355.
[9] C.S. Ray, D.E. Day, Ceram. Transact. 30 (1992) 207.
[10] A. Marotta, A. Buri, Thermochim. Acta 25 (1978) 155.
[11] C.S. Ray, D.E. Day, J. Am. Soc. 80 (1997) 3100.
[12] M. Ade et al, Zeitschrift f. Krist. (Suppl. issue) 16 (1999) 177.
[13] T.J.W. De Bruijn, W.A. De Jong, P.J. Van der Berg, Thermochim. Acta 45 (1981) 315.
[14] H. Yinnon, D.R. Uhlmann, J. Non-Cryst. Sol. 54 (1983) 253.
[15] H.E. Kissinger, J. Res. NBS 57 (1956) 21.
[16] X.J. Xu, C.S. Ray, D.E. Day, J. Am. Ceram. Soc. 74 (1991) 909.
[17] H.G. Bohn et al., J. Mater. Res. 2 (1987) 107.
[18] T. Ozawa, Polymer 12 (1971) 150.
[19] A. Marotta, A. Buri, F. Branda, J. Mat. Sci. 16 (1981) 341.
[20] R.L. Takhor, Am. Ceram. Soc. (1971) 166.
[21] M. Monthioux, O. Delverdier, J. Eur. Ceram. Soc. 16 (1996) 721.
[22] H.-P. Martin, Ph.D. Thesis, Freiberg, 1993.
[23] P. Greil, J. Eur. Ceram. Soc. 6 (1990) 53.
[24] B. Schneider et al., J. Mat. Sci. 33 (1998) 535.

[25] N.S. Jacobson, J. Am. Ceram. Soc. 76 (1993) 3.
[26] Gmelin Handbook, Si Suppl., vol. B2, p. 277.
[27] V. Heera, W. Skorupa, Mat. Res. Soc. Symp. Proc. 438 (1997) 241.
[28] T. Sakata et al., J. Electron. Microsc. 41 (1992) 185.
[29] A. Höfgen et al., J. Appl. Phys. 84 (1998) 1.
[30] O. Delverdier et al., High Temp. Chem. Proc. 1 (1992) 139.
[31] O. Delverdier et al., J. Eur. Ceram. Soc. 12 (1993) 27.
[32] R. Richter et al., Appl. Organomet. Chem. 11 (1997) 71.
[33] B.S. Mitchell et al., J. Am. Ceram. Soc., accepted